



Dynamic simulation of muscle and articular properties during human wide jaw opening

C.C. Peck ^{a,*}, G.E.J. Langenbach ^b, A.G. Hannam ^a

^a Faculty of Dentistry, University of British Columbia, 2199 Wesbrook Mall, Vancouver, BC, Canada V6T 1Z3

^b Department of Functional Anatomy, Academic Center for Dentistry (ACTA), Meibergdreef 15,
1105 AZ Amsterdam, The Netherlands

Accepted 16 May 2000

Abstract

Human mandibular function is determined in part by masticatory muscle tensions and morphological restraints within the craniomandibular system. As only limited information about their interactions can be obtained in vivo, mathematical modeling is a useful alternative. It allows simulation of causal relations between structure and function and the demonstration of hypothetical events in functional or dysfunctional systems. Here, the external force required to reach maximum jaw gape was determined in five relaxed participants, and this information used, with other musculoskeletal data, to construct a dynamic, muscle-driven, three-dimensional mathematical model of the craniomandibular system. The model was programmed to express relations between muscle tensions and articular morphology during wide jaw opening. It was found that a downward force of 5 N could produce wide gape in vivo. When the model's passive jaw-closing muscle tensions were adjusted to permit this, the jaw's resting posture was lower than that normally observed in alert individuals, and low-level active tone was needed in the closer muscles to maintain a typical rest position. Plausible jaw opening to wide gape was possible when activity in the opener muscles increased incrementally over time. When the model was altered structurally by decreasing its angles of condylar guidance, jaw opening required less activity in these muscles. Plausible asymmetrical jaw opening occurred with deactivation of the ipsilateral lateral pterygoid actuator. The model's lateral deviation was limited by passive tensions in the ipsilateral medial pterygoid, which forced the jaw to return towards the midline as opening continued. For all motions, the temporomandibular joint (TMJ) components were maintained in continual apposition and displayed stable pathways despite the absence of constraining ligaments. Compressive TMJ forces were presented in all the cases and increased to maximum at wide gape. Dynamic mathematical modeling appears a useful way to study such events, which as yet are unrecordable in the human craniomandibular system. © 2000 Elsevier Science Ltd. All rights reserved.

Keywords: Human; Biomechanics; Computer simulation; Temporomandibular joint; Masticatory muscles

1. Introduction

The mandibular motions accompanying human suckling, respiration, swallowing, speech and mastication

take place in a space constrained by jaw muscle tensions, the temporomandibular joints (TMJs), ligaments, and by contacts between the maxillary and mandibular teeth (Posselt, 1952). These constraints complement functional demands and disorders may result when structural or functional adaptive capacities are exceeded (Carlsson and LeResche, 1995).

* Corresponding author. Tel.: +1-604-8223750; fax: +1-604-8223594.

While previous studies of the functioning human jaw have provided some insight into its biomechanics, the invasiveness of many experimental procedures limits the information obtainable from living persons. Although animal models are useful substitutes, inappropriate conclusions can be drawn when their data are extrapolated to human conditions, not least because the structure and function of the human jaw and joint are unique (Creanor and Noble, 1994).

Mathematical modeling is an attractive alternative in this respect, for it offers a way to deconstruct the system in question, to manipulate the variables shaping its actions, and to demonstrate behavior consistent with such experimental measures of the human condition as are available (see reviews by Storey, 1995; Hannam and Langenbach, 1995). In static modeling, the mandible is usually represented as a rigid or flexible structure acted on by variable muscle tensions and constrained from moving by reaction forces at designated sites. In dynamic modeling, the mandible is defined as a physical structure (with specific inertial properties) acted upon by forces which may be constant (e.g. gravity) or changing (e.g. act-specific muscle tensions), and the jaw is free to undergo displacement until its motion is arrested by constraining forces. Difficulties encountered in mathematical modeling include the simulation of complexly layered, multipennated masticatory muscles (see Hannam and McMillan, 1994), flexible and compressible articular discs, and mandibles capable of deformation (Koriath and Hannam, 1994a). Moreover, assigning the appropriate physical values to the various structural components is not straightforward, often requiring simplification and the use of unverified data. In fact, some desirable information may never be obtainable from living humans. Despite these limitations, recent sophisticated dynamic jaw models suggest, *inter alia*, that active and passive muscle tensions interact to cause compression of the mandibular joint during plausible jaw motions (Koolstra and van Eijden, 1995, 1996, 1997b; Langenbach and Hannam, 1999).

Perhaps the most significant limitation of present models is their inability to demonstrate plausible gapes caused by maximal activation of the inframandibular and inferior lateral pterygoid muscles. Typically, their maximum gapes have been around 35 mm, well below the reported mean of 51 mm (Szentpetery, 1993). Koolstra and van Eijden (1997b) suggest that this restricted opening might be due to over-shortening of the opening muscles, which decreases the tension of the digastrics and inferior lateral pterygoids to approximately 40 (25 N) and 50% (24 N) (Koolstra and van Eijden, 1997a) of their maximum tensions, respectively, thereby reducing their ability to overcome the passive tensions of the jaw-closing muscles. They consider that hyoid movement during opening *in vivo* (a missing factor in their simulation) would normally sustain opener-muscle

lengths adequate for the tensions needed to open the jaw widely. While this may be so, it would only apply to the digastric muscles, as the lateral pterygoids have immobile origins. Maximal gape can be reached by applying external forces of less than 10 N to the jaws of relaxed individuals with inactive digastric muscles (Lynn and Yemm, 1971). Appropriate length–tension curves in the jaw-closing muscles are necessary to accommodate jaw opening under these conditions. The same curves would also have to accommodate other jaw positions believed to be influenced or maintained by passive muscle tensions, including the mandible's gravitational rest position (Oishi, 1967; Lynn and Yemm, 1971; Yemm, 1976; Miller and Chierici, 1977). This is believed to occur at an interincisal separation of 3–5 mm (Brill and Tryde, 1974). The rest position also fluctuates 2–3 mm during recording sessions (Dibdin and Griffiths, 1975) and is influenced by low levels of mandibular elevator activity in the alert person (Kawamura et al., 1967; McNamara, 1974; Møller, 1976). In summary, plausible dynamic models should have length–tension properties assigned to closing muscles which satisfy the twin criteria of permitting gapes of 50 mm with a 10-N external force exerted on the mandible, while at the same time producing a gravity-determined jaw resting posture consistent with *in vivo* behavior. It seems likely that the jaw-closing muscles in dynamic models may require length–tension properties different from these assumed so far.

As mandibular translations and rotations cause jaw muscle attachments to move differently (Goto et al., 1995), the balance between active and passive tensions can be expected to alter dynamically during different oral functions and in response to skeletal changes (which may also alter reaction forces). The predictions of any human jaw model therefore have to be realistic for various functional acts and remain so for different boundary morphologies (e.g. different condylar guidances). An appropriate dynamic interplay between active and passive muscle tensions for a given system is critical here, as tensions are major determinants of jaw position. If this 'balance' does not occur, ligamentous or other external constraints must be invoked to control jaw motion.

In the present study, we first wished to verify the magnitude of externally applied force needed to reach maximum jaw gape in relaxed individuals [*i.e.* to confirm the suggestions made previously by Lynn and Yemm (1971)]. We then constructed a dynamic, muscle-driven mathematical jaw model that could duplicate both this act and a plausible, gravitational resting posture. We postulated that these twin requirements might require modification of the passive length–tension curves used in previous studies. On the premise that we could design such a model, our next aim was to determine whether muscle tensions alone (in the ab-

sence of ligamentous or similar passive restraints) could restrain jaw motion during wide midline opening, and during opening with a lateral deviation. Finally, we were interested in whether the model remained stable when systematic alterations were made to articular morphology.

2. Methods

2.1. Determination of forces required to attain wide gape

To confirm the behavioral variables associated with externally induced jaw opening, we measured the magnitude and angle of the force needed to attain maximum gape in five healthy adults (four males, one female; age range 25–31 years). In each participant, a customized acrylic clutch, retained on the lower dental arch by extensions into the embrasures and beyond the buccal dental undercuts, provided a rigid platform over the mandibular dentition. A 10-cm shaft, extending from a hand-held digital force gauge (Accuforce Cadet; Ametek, Largo, FL), was fixed to the clutch with a universal joint in the dental midline and 1 cm anterior to the incisors. This allowed the mandible to be pushed

or pulled with a known force in any direction on the midsagittal plane. Markers, in the form of calibrated, linear scales, were attached separately to the mandibular clutch, the force gauge's shaft, and a cranially supported spectacle frame worn by the participant. The relative positions and orientations of these markers were recorded continuously with a fixed video camera (Hi8 VM-H38A; Hitachi-Canada, Quebec) aligned with its optical axis perpendicular to the parasagittal plane.

The recording sessions were performed in an isolated room. Each participant was seated in a slightly reclined dental chair, and trained to relax. With a restraining hand on the participant's forehead, the operator then slowly depressed the mandible by means of the force gauge until maximum gape was attained. Throughout the movement, the operator used the camera's microphone to record verbally (and continuously) the value of the force displayed digitally on the gauge. In this way, cranial, jaw and force-gauge shaft positions and orientations were correlated with the applied force.

After each recording session, single video frames at the beginning and end of opening were digitized via a UNIX-based workstation (IRIS Capture 1.3.3; SGI, Mountain View, CA). Screen pixel co-ordinates corresponding to all scale markers were extracted individually from these images (IRIS ImgView 2.1; SGI). The marker positions were used to calculate (i) the linear distance traveled during opening by the shaft's attachment site on the clutch, and (ii) the direction of the applied force (i.e. the orientation of the shaft) relative to the occlusal plane. For each individual participant the mean direction and magnitude of applied force for the sample of five participants was used to guide the determination of passive muscle tensions in the dynamic model (see below).

2.2. Definition of the jaw model

The model was based on previously published descriptions of musculoskeletal geometry (Baron and Debussy, 1979) and muscle physical properties (van Eijden and Raadsheer, 1992; van Eijden et al., 1995, 1996, 1997). It allowed six degrees-of-freedom motion shaped by forces from 16 craniomandibular muscle groups, two temporomandibular joints, and gravity (Fig. 1). We developed it with commercially available software written specifically for the design, visualization and analysis of dynamic models common in mechanical engineering (ADAMS; MDI, Ann Arbor, MI). We ran the program on an Indy RS4000 workstation (SGI). ADAMS employs a widely used method for dynamic analysis (van den Bogert and Nigg, 1999), in which the jaw system was defined as a collection of mixed non-linear differential and algebraic equations. Numerical integration of the jaw and muscle accelerations in these equations calculated their velocities and positions. In

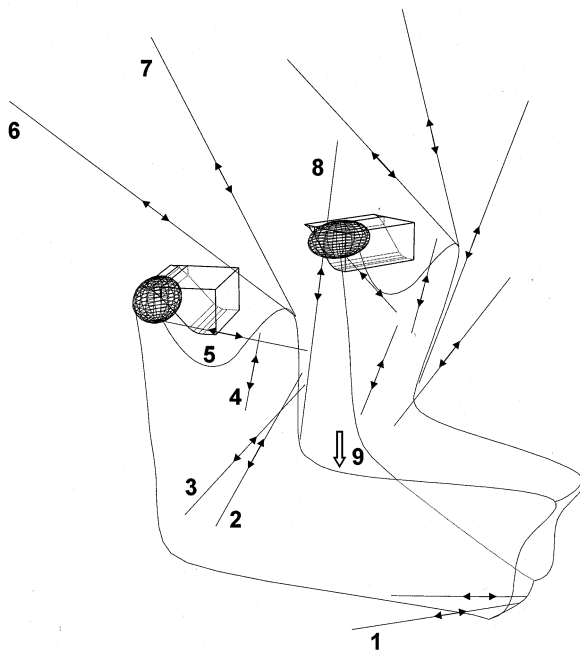


Fig. 1. Anterolateral view of the basic model showing the muscle group actuators' lines of action. Muscle groups, 1-anterior digastric; 2-superficial masseter; 3-medial pterygoid; 4-deep masseter; 5-lateral pterygoid; 6-posterior temporalis; 7-middle temporalis; 8-anterior temporalis. 9-direction of gravitational field.

brief, this involved a two-phase predictor–corrector technique whereby initially a solution was estimated at a point in time in the analysis by fitting a polynomial through solutions at previous points in time and extrapolating forward. To improve upon this predicted solution, a corrector phase was implemented where time was held constant temporarily and the predicted solution was iteratively improved with the numerical integration algorithm. These iterations continued until either differences in successive iterations were below a user-defined tolerance (in our case 10^{-6} of the earlier iteration), or the user-specified number of iterations (in our case 10) had been performed. If the difference fell below our tolerance, because the corrector had converged all displacement variables to within the tolerance before the number of iterations had been performed, then the solution was accepted, and the process continued by initiating another predicted solution at a step forward in time. If the specified number of iterations had occurred, the predicted solution had not converged and was rejected. The predictor–corrector technique then backed up to a point in time closer to the previous acceptable time-step than that just used in the failed estimate. In addition, the order of the polynomial used to predict a solution was also reduced to help find an acceptable solution.

2.3. Mandible and dentition

The mandible was defined as a rigid body with a mass of 200 g. It was located in the midline (10 mm below the second molar bite-point) and had the following moments of inertia: I_{xx} , 92.2; I_{yy} , 182.2; and I_{zz} , 125.2 kg m². These properties were derived from a finite-element model of an intact human jaw previously developed in our laboratory (see Langenbach and Hannam, 1999). The mandible was positioned in a gravitational field of 9.8 m/s² to simulate a head in upright posture. The dentition was represented by flat maxillary and mandibular occlusal planes without cusps. Vertically directed reaction forces on the mandibular teeth (1000 N/mm) simulated the occlusal interface and prevented further jaw closing.

2.4. Temporomandibular joints

The joints were ellipsoidal, canted condylar shapes that rotated and slid against frictionless, curvilinear surfaces (Fig. 2). Each condyle measured 20 mm medio-laterally, 10 mm superoinferiorly and 10 mm antero-posteriorly (Öberg et al., 1971). We used physical constants to define the resistance, i.e. the functional boundary, formed by each articular fossa and its disc. To provide a typical curvilinear condylar path, the lateral profile of this boundary was represented by the function, $y = 5 \times \cos(x/13 \times \pi) - 5$, where x and y were

the anteroposterior and superoinferior co-ordinates, in mm, respectively. This boundary consisted of seven contiguous plates with typical anterior, inferior and lateral dimensions of 19, 10 and 24 mm, respectively (Solberg et al., 1985), and a condylar path inclination of approximately 40° to the occlusal plane (Lundeen et al., 1978). The sagittal-plane inclination of each fossa–disc boundary was 20° to the midsagittal plane, so the medial pole of the condyle was posterior to the lateral pole (Yale et al., 1966). To investigate the relation between structure and function, a similar pair of joints was developed, except that the condylar-path inclination in each was reduced to 25° relative to the occlusal plane (Fig. 2).

Each condyle was monitored for contact with its functional fossa–disc boundary by finding intersections between the objects' geometries. When contact was detected, and if the computed post-contact velocity was below a nominal 1 mm/s, then contact between the two bodies was assumed to be persistent. If contact was intermittent, an impulse-based, momentum–balance computation was performed, which resulted in the objects separating with an instantaneous change in velocity, i.e., they collided and rebounded. In the constant-contact case, an instantaneous constraint was applied between the two objects, but if the force at the constraint indicated the objects were trying to separate, the constraint was removed. As material properties were unavailable for these combined bone–collagen objects, we assigned values previously described for bone and fibrocartilage, i.e. we used a Young's modulus of elasticity, Poisson's ratio and density of 0.2 GPa, 0.35 and 1.8 g/cm³, respectively (Wong and Carter, 1988; Dechow et al., 1993). The value for the coefficient of restitution was one, denoting an elastic collision, with conservation of momentum and energy. Each condyle could be distracted freely from its boundary, and there were no ligamentous or soft tissue constraints.

2.5. Muscles

The masseter, temporalis, medial and lateral pterygoid and digastric muscles were divided into 18 functional groups for which physiological data were available. The jaw-closing muscles were represented by anterior, middle and posterior temporalis, superficial and deep masseter, and medial pterygoid groups. The opening muscles were represented by anterior digastric and lateral pterygoid (inferior head) groups. The muscles (and their subgroups) were simulated with Hill-type, flexible, single-line actuators (Zajac, 1989). Each had a fibre and a tendon component, together producing active and passive tensions. Apart from the digastric muscle, all muscle attachment sites were derived from the work of Baron and Debussy (1979), which

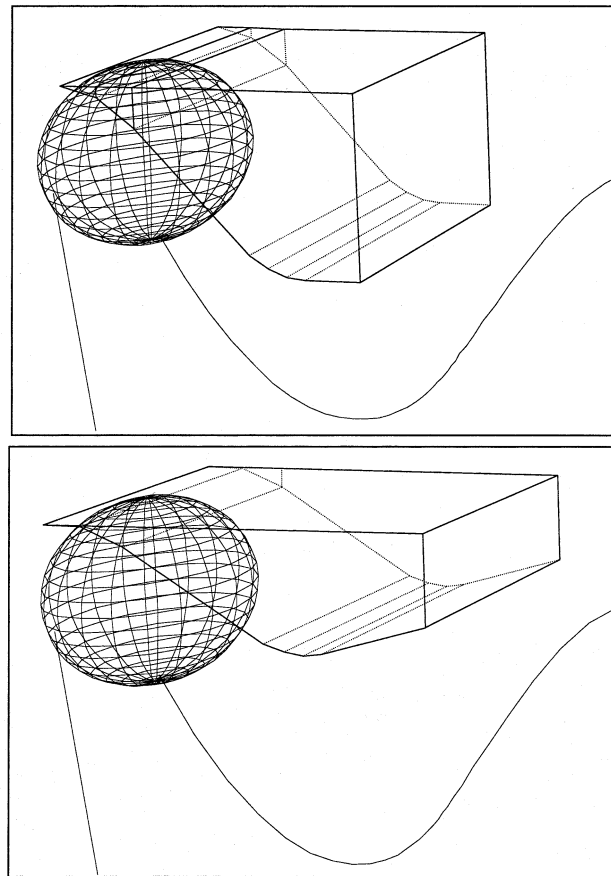


Fig. 2. TMJ analogues 40° condylar guidance (upper) and 25° condylar guidance (lower).

was based on five human skulls. The actuator orientations represented the central axis of the body of each muscle or subgroup from origin to insertion (Fig. 1). We found it necessary to damp each muscle actuator (10 Ns m) to prevent high-frequency internal oscillations. We considered that this represented the muscle and other soft tissue viscosity likely to be present in vivo, such as a muscle's increasing passive resistance to faster movements and decreasing passive forces (muscle relaxation) when its length is held constant (Winters, 1990).

Special consideration was given to the digastric muscle, because its line of action is influenced by the position of the hyoid bone. The hyoid changes position during function (Winnberg, 1987; Winnberg et al., 1988; Haralabakis et al., 1993; Hiimae et al., 1995) with a weak correlation relative to the mandible in its closed and maximum open positions (Muto and Kanazawa, 1994). The angle between the mandibular plane and hyoidale varies between 10 and 17° during jaw opening (Pancherz et al., 1986; Winnberg et al., 1988), but to simplify the model we chose a fixed line of

action for the digastric actuator, which was 15° to the mandibular plane.

2.6. Specification of muscle fibre/tendon ratios

A major requirement for the model was its ability to provide a full range of typical jaw motion under the influence of muscle forces. During its construction, therefore, we utilized kinematic data to define the jaw's extreme range of motion, i.e. we produced typical border movements, as described by Posselt (1968), at the mandibular incisor and condyles (Fig. 3). Invariably, these simulations showed that at the position of wide gape, all jaw-closing muscles attained their individual maximum lengths. We set the maximum length for all closing muscles nominally at 150% of their optimal length, in accord with typical maximum values for skeletal muscle (Zajac, 1989). Although the ranges of motion vary between different muscles, and indeed between individuals for the same muscle (Brown et al., 1996), setting maximum lengths for the closing muscles to less than 150% would have produced optimal lengths

at a wider gape. In this way, we provided optimal conditions for our model to attain a typical mandibular rest position (with minimal freeway space) derived solely from passive muscle tensions (see below).

With the jaw at maximum gape [i.e. an interincisal opening of 50 mm, and a sagittal-plane rotation of 30°; Salaorni and Palla (1994), Peck et al. (1997)], we calculated the lengths of the muscle fibre and tendon components which would enable each muscle to reach its total length at maximum gape, while retaining fibre, tendon and sarcomere length ratios consistent with the literature (van Eijden and Raadsheer, 1992; van Eijden et al., 1995, 1996, 1997). For these calculations, all length changes were assumed to occur within the fibre component. Tendons were modeled as inextensible elements because their functional lengths reportedly change by less than 4% (Curwin and Stanish, 1984). Components calculated this way meant that, when the jaw was in the intercuspal position, sarcomere lengths averaged 9% less than the 2.73 µm previously assumed to be optimal (Muhl et al., 1978). The properties are summarized in Table 1.

2.7. Specification of muscle tension properties

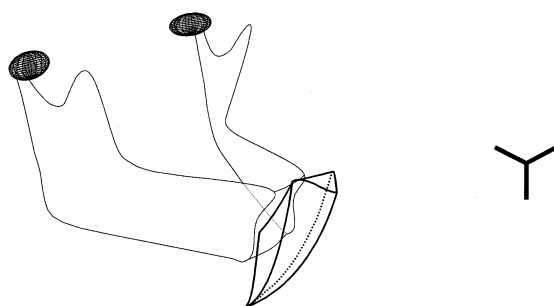
2.7.1. Passive muscle tensions

Each muscle's passive tension, F_p , was represented by the function:

$$F_p = \frac{(e^{(\text{musclelength}/\text{max_musclelength})\text{exp}} - 1)(F_{\text{max}} \times \text{factor})}{(e^{\text{exp}} - 1)},$$

i.e. passive tension increased exponentially with increasing muscle length (Hill, 1953; Gordon et al., 1966; Woittiez et al., 1983). The maximum muscle length, max_musclelength , was derived from the kinematic model's data (Fig. 3; Table 1), and is expressed as the length change beyond optimal length. Maximum passive muscle force, F_{max} , and scaling factor, factor , were derived as outlined below. The exponent was raised to the power of exp to change the slope of the exponential function, and consequently the rate which passive tension developed with respect to muscle length. This rate variable was altered when we were determining the jaw model's rest position.

Passive force began to increase at optimal muscle length ($\text{musclelength} = 0$), and was greatest at maximum length ($\text{musclelength} = \text{max_musclelength}$). Its maximum (F_{max}) was proportional to the muscle's cross-sectional size and was determined by multiplying the muscle's physiological cross-sectional area (PCS) with an appropriate constant (Ikai and Fukunaga, 1968; Pruim et al., 1980; Nygaard et al., 1983; Weijs and Hillen, 1985; Fitts et al., 1991). Thus, for each muscle, $F_{\text{max}} = \text{PCS} \times 40 \text{ N/cm}^2$. The PCS were obtained from whole muscle cross-sections (Weijs and Hillen, 1984a,b) according to proportions derived by Nelson (1986) (Table 1). To assign an appropriate length–tension curve to each muscle, each of the elevator's F_{max} was scaled by an identical factor in the following manner. We constructed a parametric jaw model with ADAMS, in which we specified this factor as the design variable.



MOVEMENT	CONDYLAR MOTION	INCISOR MOTION
Protrusion	10 mm anterior translation; 0° sagittal plane rotation	10 mm anterior translation
Opening following protrusion	6 mm anterior translation; 30° sagittal plane rotation	50 mm vertical translation
Hinge-opening	0 mm anterior translation; 13° sagittal plane rotation	20 mm vertical translation
Opening following hinge-opening	16 mm anterior translation; 17° sagittal plane rotation	30 mm vertical translation
Normal opening	16 mm anterior translation; 30° sagittal plane rotation	50 mm vertical translation
Laterotrusion	Balancing condyle: 8 mm anterior translation Working condyle: 4° horizontal plane and 1.7° frontal plane rotation	12 mm antero-lateral translation
Mediotrusion following laterotrusion	Balancing condyle: 2 mm anterior translation Working condyle: 10 mm anterior translation	12 mm antero-medial translation
Opening following laterotrusion	Working condyle: 16 mm anterior translation, Balancing condyle: 8 mm anterior translation; 30° sagittal plane rotation	50 mm vertical translation

Fig. 3. Incisal point envelope of border movements produced by the kinematically driven model (border movement pathways to the right have been omitted for clarity). Calibration bar, 12 mm.

Table 1
Muscle properties

Muscle group	Muscle-length IP ^a (mm)	Muscle length-WG ^b (mm)	Sarcomere length-IP ^a (μ m)	Tendon (% muscle length)-IP ^a	Tendon length (mm)	Proportion of whole muscle (%)	PCS ^c (cm ²)	F_{\max}^d (N)	Active tone at RP ^e (N)	Passive tension at WG ^b (N)
Superficial masseter	51.46	66.88	2.63	46	23.67	70	4.76	190.4	0.35	2.28
Deep masseter	29.07	44.85	2.32	29	8.40	30	2.04	81.6	0.15	0.98
Medial pterygoid	40.51	50.63	2.41	64	26.09	100	4.37	174.8	0.31	2.10
Anterior temporalis	75.54	95.92	2.66	50	37.77	48	3.95	158.0	0.28	1.90
Middle temporalis	65.81	93.36	2.27	48	31.59	29	2.39	95.6	0.17	1.15
Posterior temporalis	77.11	101.08	2.51	51	39.17	23	1.89	75.6	0.14	0.91
Lateral pterygoid						70	1.67	66.9		
Anterior digastric						100	1.00	40.0		

^a Intercuspal jaw position.

^b Wide gape jaw position.

^c Muscle physiological cross-section area.

^d Maximum muscle tension.

^e Rest position of the jaw.

Table 2

Jaw models' structural (condylar guidance) attributes and functional (muscle tension variable) alterations to meet specific objectives

Model	Condylar guidance (°)	Muscle tension variables	Objective
40RP	40	Jaw-closer muscle passive tension curve, and if needed jaw-closer muscle active tone	Determination of clinical mandibular rest position
40LF	40	Jaw-opener activity expressed as simple linear force–time function	Symmetrical jaw opening to wide gape
40XF	40	Jaw-opener activity expressed as expanded linear force–time function	Improved symmetrical jaw opening to wide gape
25PF	25	Jaw-opener activity expressed as previous model's (model 40XF) expanded linear force–time function	Symmetrical jaw opening to wide gape
25LF	25	Jaw-opener activity expressed as simple linear force–time function	Symmetrical jaw opening to wide gape
25XF	25	Jaw-opener activity expressed as expanded linear force–time function	Improved symmetrical jaw opening to wide gape
40LF(As)	40	Jaw-opener activity expressed as simple linear force–time function and left lateral pterygoid muscle actuator deactivated	Asymmetrical jaw opening to extreme lateral position

Factor was changed incrementally in a series of analyses, until passive length–tension curves were found which enabled the jaw (with an externally applied force as determined above from our experiment on five healthy adults, and in the presence of gravity) to reach stable equilibrium at a maximum gape of 50 mm.

2.7.2. Active muscle tensions

Each muscle's maximum possible active tension also depended on its cross-sectional size, i.e. F_{\max} . However, the instantaneous active tension actually developed in each muscle as a consequence of neural drive was expressed by the linear function:

$$F = F_1 \times t_1,$$

where F_1 is the greatest force generated by the actuator for the task, and is $\leq F_{\max}$, and t_1 is time of actuator activity.

In an attempt to improve the opening trajectory of the model for muscle-activated midline jaw opening, the function expressing the digastric and/or lateral pterygoid actuator activity was then expanded to:

$$F_t = F_1 \times t_1 + F_2 \times t_2 \dots + F_n \times t_n,$$

where F_1 , original force as above, and $F_{2\dots n}$, additional force applied at time $t_{2\dots n}$ and $t_0 < t_1 < t_2 < \dots t_n < t_f$.

2.8. Jaw dynamics

For the model and its modifications (Table 2), correlated dynamic properties were obtained, including predictions of loads between the condyles and disc/fossa boundaries, passive and active tensions in the muscle actuators, and displacements at the mandibular incisor and condyles.

2.9. Determination of the mandibular rest position (model 40RP)

To determine the rest position, we allowed the model described above to reach a state of equilibrium, influenced by gravity and passive muscle tensions alone. In this model (40RP; see Table 2), we altered the variable *exp* in the passive tension function for each muscle in an attempt to reach the target rest position of an interincisal opening of 3–5 mm (Brill and Tryde, 1974). We postulated that if the jaw stabilized at a wider interincisal separation than this, it would be necessary to add steady-state active drive to all jaw-elevator actuators to achieve an acceptable rest position. Under these circumstances, any additional active muscle 'tone' was specified as a constant fraction of each muscle's F_{\max} . It was determined by parameterizing the model with tone as the design variable and increasing this variable incrementally in a series of analyses until a typical rest position was achieved.

2.10. Muscle-activated midline jaw opening (models 40LF and 40XF)

2.10.1. Use of linear force–time functions for active muscle tensions (model 40LF)

We coactivated the digastric and lateral pterygoid actuators on the above model to simulate jaw opening (model 40LF; see Table 2). An optimization technique was performed to determine these actuator forces (modified method of feasible directions (ADAMS, 1994)). A parametric model was defined by specifying digastric and lateral pterygoid actuator forces as design variables. Screening analyses were performed in which

these design variables were systematically altered between 0 force and F_{\max} . In this way, we determined a 5–10 N ‘window’ within which each actuator would have to work when opening the jaw to maximum gape (50 ± 5 mm interincisal separation) in approximately 1 s, against passive tensions in the jaw-closing actuators. Our objective was jaw opening at a rate as close as possible to 2° rotation per mm of anterior condylar translation in the sagittal plane (Salaorni and Palla, 1994). This was expressed as the objective function, $\Sigma \sqrt{(R/T - 2)^2}$, where R_{is} , sagittal plane jaw rotation, and T_{is} , anterior condylar translation at each time step of the model simulation from intercuspal position to wide gape. We then invoked the optimization algorithm to drive the actuators within the range determined by our screening analyses, so that this objective function was minimized and the function’s derivative approached 0. This algorithm was constrained to a maximum interincisal gape between 48 and 52 mm, with an opening duration of 0.5–1 s.

2.10.2. Use of expanded linear force–time functions for active muscle tensions (model 40XF)

Once the model had been optimized as above, we attempted to obtain a better opening trajectory by selectively adding digastric and/or lateral pterygoid actuator activity at points along the opening path where condylar rotation/translation varied by $\pm 0.5^\circ/\text{mm}$ from our objective of $2^\circ/\text{mm}$ (model 40XF; see Table 2). We determined additional actuator activity with the same procedure, namely a screening analysis, followed by optimization, on successive increments of the opening path.

2.11. Opening with reduced condylar guidance (models 25PF, 25LF and 25XF)

These models were developed to observe the effect of altered structural guidance by the articulation. Here, the anteroinferior inclination of the condylar path was reduced to approximately 25° relative to the occlusal plane (Fig. 2). To achieve this, the disc/fossa boundary of the original model was rotated 15° upwards in the sagittal plane. In other respects, the initial model (model 25PF; see Table 2) was identical to model 40XF, including the model’s digastric and lateral pterygoid actuator activity, and wide jaw opening was attempted. To obtain a more typical opening trajectory, we again followed the sequence outlined above; a new model (25LF) was constructed with linear force–time functions for the active muscle tensions, and another (25XF) constructed with expanded linear force–time functions for the active muscle tensions. These force functions were computed by the same procedure as above, i.e. design studies, followed by optimization to minimize the objective function.

2.12. Asymmetrical opening (model 40LF – As)

We constructed this model to observe the effect of an altered function on the system. We changed the task to asymmetrical jaw opening (still without ligamentous constraints). It was identical to model 40LF, with the original anteroinferior condylar path inclination of 40° , and utilized linear force functions for the opener actuators. In this case, however, the left lateral pterygoid actuator was deactivated so that the jaw moved to the left during opening (model 40LF – As).

3. Results

3.1. Forces required to attain wide gape in vivo

Our measurements of the force needed to attain wide gape in relaxed, conscious individuals indicated that maximum, passively guided gapes in excess of 45 mm could be achieved with an applied external force of 5.0 ± 0.4 N at $83 \pm 2^\circ$ (mean \pm S.D.) to the occlusal plane. Individual forces were, 4.5, 4.5, 5.1, 5.3, 5.5 N at 87° , 81° , 81° , 82° , 84° , respectively, to the occlusal plane, confirming the conclusions of Lynn and Yemm (1971) that forces well under 10 N were sufficient to open the relaxed jaw fully. For modeling purposes, therefore, we specified that the jaw should be able to reach an interincisal wide gape of 50 mm when a downward and backward directed force of 5 N was applied to the lower incisors at 83° to the occlusal plane.

3.2. Definition of the jaw model

3.2.1. Specification of passive muscle-tension properties

At wide gape, the maximum passive tension in each of the muscles was calculated to be 1.2% (defined as *factor* in the passive muscle-tension function) of each muscle’s F_{\max} (Table 1). With these passive tensions in the jaw-closing actuators, gravitational force, and a 5 N vertically directed force applied to the model, equilibrium was achieved at wide gape. The generic passive muscle length–tension curve used is seen in Fig. 4, and examples of passive force–length relations generated by the jaw elevators in the different models are shown in Fig. 10.

3.3. Jaw dynamics

3.3.1. Determination of the mandibular rest position

Under the influence of gravity and passive muscle tension alone, model 40RP reached rest positions (measured at the mandibular incisor) between 11 and 38 mm, when the *exp* variable (which determines the slope of the exponential function) ranged from 10 to 0.0001 (Fig. 5). As values of *exp* below 0.1 caused only minor

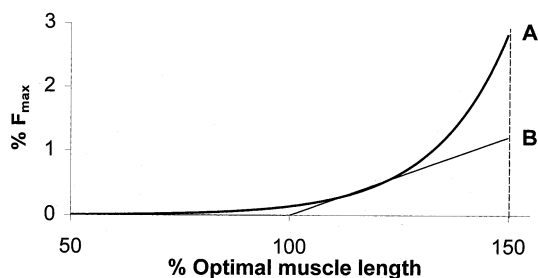


Fig. 4. Generic passive muscle length–tension curve utilized for all muscle group actuators in (A) previous studies⁸, and (B) current study. Muscle length is scaled to optimal muscle length, l_0 , on abscissa. Muscle tension is scaled to maximum tetanic muscle tension F_{\max} , on ordinate. Dotted line represents our nominally set maximum functional muscle length. Note at this length, passive muscle tensions are greater in A (2.8% F_{\max}) than in B (1.2% F_{\max}) (⁸Koolstra and van Eijden, 1997a,b).

reductions in rest position, we selected this *exp* value, which provided a rest position gape of 11 mm. To reduce this rest-position gape to our target 3–5 mm interincisal opening, we had to add active tone to each of the jaw-closing muscle actuators. This corresponded to 0.18% of each muscle's F_{\max} (Table 1).

3.4. Muscle-activated midline jaw opening

3.4.1. Use of linear force–time functions for active muscle tensions (model 40LF)

To simulate a plausible wide gape caused by activation of the jaw-opening muscles, the screening analyses initially performed on model 40LF reduced the active tensions in the jaw-opening actuators from their maxi-

imum range (0 N– F_{\max}) to a range of 2–6 N for the digastric actuators, and 8–12 N for the lateral pterygoid actuators. To achieve typical jaw opening to wide gape, these actuator values were used by the optimization algorithm to open the jaw at a rate of 2° sagittal-plane jaw rotation per mm of anterior condylar translation. The optimized digastric and lateral pterygoid actuators' force functions were $F_{\text{DG}} = 3.2 \times t_1$ and $F_{\text{LP}} = 10.1 \times t_1$, respectively (Fig. 9a). With these functions, wide gape was attained in 0.95 s, and tension in the lateral pterygoid was more than three times that in the digastric, the actuators reaching maximal forces of 9.6 and 3.0 N, respectively. Apart from the posterior temporalis, which reached a maximum of 7.0 N, all passive muscle tensions were relatively low during the opening movement, with values less than 2.5 N (Fig. 10a; Table 3). Condylar loading increased as the jaw opened and peaked at 15.8 N at wide gape (Fig. 12; Table 3).

At various points along the opening path, model 40LF deviated by more than $\pm 0.5^\circ/\text{mm}$ from our objective of $2^\circ/\text{mm}$, and indeed this objective was not reached until 0.48 s (17 mm incisal opening) after opening commenced (Fig. 11). Although wide gape was attained with these optimized actuator functions, the trajectory of the mandibular mid-incisor point in opening displayed a marked translatory component at approximately two-thirds gape (Fig. 6). This movement coincided with the condyle's transition from the relatively vertically oriented posterior wall to the horizontally oriented crest of the eminence of the disc/fossa boundary. At this transition point, the condylar forces had increased to a maximum of 8.8 N, then remained relatively constant as the condyle negotiated the eminence's crest, and finally increased with further gape.

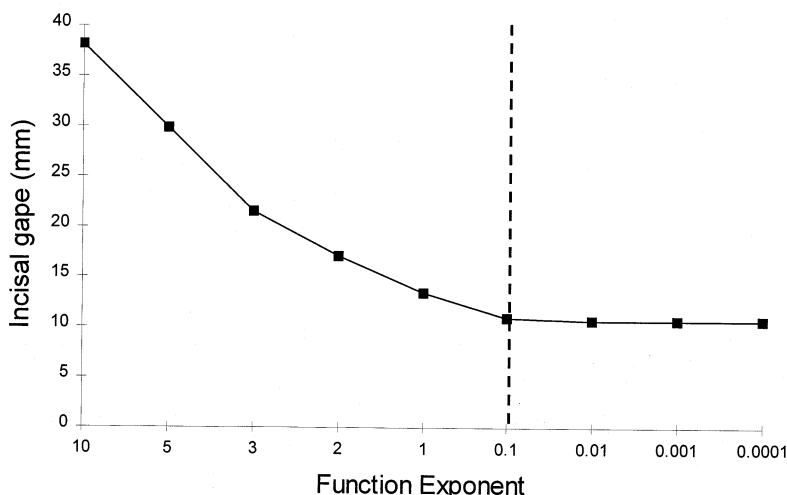


Fig. 5. Comparison of rest position incisal gape for passive muscle tension function exponents between 10 and 0.0001. The dotted line indicates exponents beyond which there was little effect on incisal gape.

Table 3

Jaw motions, joint loads and muscle tensions at wide gape (models 40XF and 25XF) and at maximum left lateral jaw deviation (model 40XF–As)

Model 40XF		Model 25XF	Model 40XF – As	
			Right (balancing side)	Left (working side)
TMJ load (N)	28	10.7	7.3	4.1
Incisal gape (mm)	50	48	27 (lateral, 11; inferior, 21)	
Sagittal plane jaw rotation (°)	30	33	14 (frontal, 3; horizontal, 4.5)	
Opening duration (s)	0.60	0.68	0.6	
<i>Maximum opening muscle tensions (N)</i>				
Lateral pterygoid	16.8	6.4	6.1	0.0
Digastric	11.6	3.4	1.9	1.9
<i>Maximum closing muscle tensions (N)</i>				
Superficial masseter	4.5	2.0	2.0	1.6
Deep masseter	4.4	0.8	0.7	0.3
Medial pterygoid	2.3	1.7	1.3	4.5
Anterior temporalis	4.3	1.7	1.3	0.8
Middle temporalis	10.1	1.2	0.5	0.2
Posterior temporalis	4.6	1.0	0.4	0.1

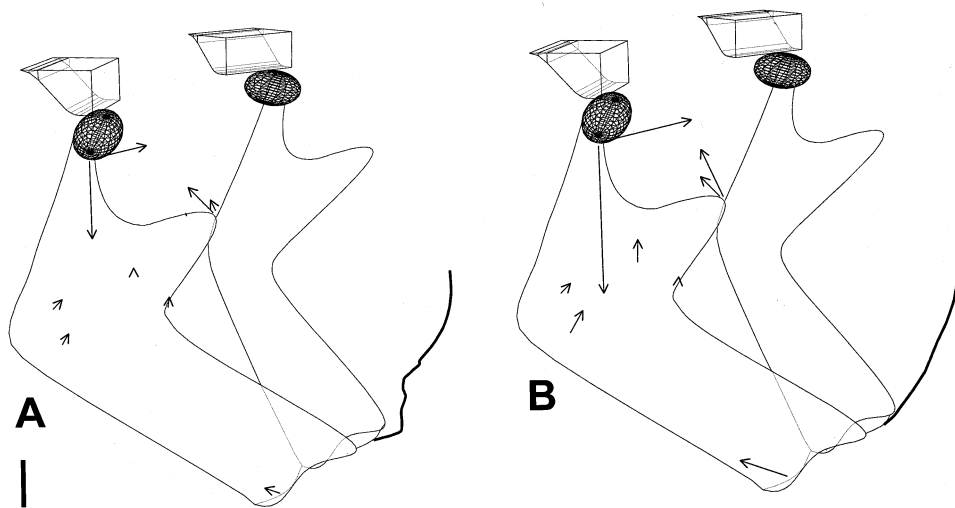


Fig. 6. Effect of simple and expanded linear jaw-opener muscle activity on incisor opening pathway for 40° condylar guidance models. Anterolateral view of (A) model 40LF, and (B) model 40XF including muscle vectors (shown on the right side only) at wide gape. Bold line represents mandibular incisor opening pathway. Calibration bar, 10 N (force vectors) or 12 mm (incisal displacement).

3.4.2. Use of expanded linear force–time functions for active muscle tensions (model 40XF)

To improve the opening trajectory of model 40LF, we selectively added digastric or lateral pterygoid actuator activity when the objective function deviated by more than 0.5°/mm from our objective of 2°/mm. As the optimized objective function from model 40LF did not reach its goal of 2°/mm until 0.48 s of opening, we optimized the model for the initial 0.25 s of opening. It

was then necessary to add additional lateral pterygoid actuator activity at 0.2, 0.4 and 0.54 s, and to add additional digastric actuator activity at 0.48 and 0.58 s. The resulting jaw trajectory and objective function can be seen in Figs. 6 and 11, respectively; the final optimized, expanded linear functions for the lateral pterygoid and digastric actuators are presented in Table 4 and Fig. 9a. With these functions, wide gape of 50 mm was attained in 0.6 s, with the digastric and lateral

pterygoid actuators reaching maximal forces of 11.6 and 16.8 N, respectively. Apart from the passive tension of the middle temporalis (which reached a maximum of 10.1 N), all passive tensions remained below 4.6 N throughout the opening movement (Fig. 10b; Table 3). These maxima coincided with maximum gape. The TMJs were compressively loaded throughout the opening movement: individual joint forces increased to a maximum of 28 N at 44 mm, and remained at this force level to wide gape (Fig. 12).

3.5. Opening with reduced condylar guidance

In our first attempt at jaw opening with reduced condylar-guidance angles, we used the expanded linear force–time functions from model 40XF to define activity in the jaw-opening actuators. This model (25PF)

attained a gape of only 34 mm and a sagittal-plane jaw rotation of 24°, at which point the condyles had translated beyond their anterior limit of 20 mm in 0.48 s. The objective function resulting from this simulation did not approach the goal of 2° sagittal-plane jaw rotation per mm of anterior condylar translation.

In our next attempt to simulate a plausible wide gape with reduced condylar guidance, we initially used linear actuator force functions (model 25LF), in which the optimized digastric and lateral pterygoid actuators' forces were $F_{DG} = 3.0 \times t_1$ and $F_{LF} = 6.0 \times t_1$, respectively (Fig. 9b). Here, a wide gape of 50 mm was attained in 0.87 s (Fig. 7), and tension in the lateral pterygoid was twice that in the digastric, with the actuators reaching maximal forces of 5.2 and 2.6 N, respectively (Figs. 7 and 9b). All passive muscle tensions were relatively low during the opening movement,

Table 4
Expanded linear force functions assigned to the (A) lateral pterygoid actuator, and (b) digastric actuator for the 40 (model 40XF) and 25° (model 25XF) condylar guidance models^a

Model 40XF		Model 25XF	
<i>(A) lateral pterygoid actuator function</i>			
$F_t = \text{time}_0 \times 11 + \text{time}_{0.2} \times 3.7 + \text{time}_{0.4} \times 10$ + $\text{time}_{0.54} \times 140$	For $0 \leq \text{time} < 0.59$ s	$F_t = \text{time}_0 \times 6 + \text{time}_{0.19} \times 2$ + $\text{time}_{0.51} \times 10$	For $0 \leq \text{time} < 0.66$ s
$F_t = 16.8$ N	For $\text{time} \geq 0.59$ s	$F_t = 6.4$ N	For $\text{time} \geq 0.66$ s
<i>(B) digastric actuator function</i>			
$F_t = \text{time}_0 \times 4 + \text{time}_{0.48} \times 16 + \text{time}_{0.58} \times 500$	For $0 \leq \text{time} < 0.59$ s	$F_t = \text{time}_0 \times 3 + \text{time}_{0.33} \times 0.5$ + $\text{time}_{0.63} \times 40$	For $0 \leq \text{time} < 0.66$ s
$F_t = 11.6$ N	For $\text{time} \geq 0.59$ s	$F_t = 3.4$ N	For $\text{time} \geq 0.66$ s

^a F_t , actuator force at time, t ; time_n , time (n s) when onset of force occurs.

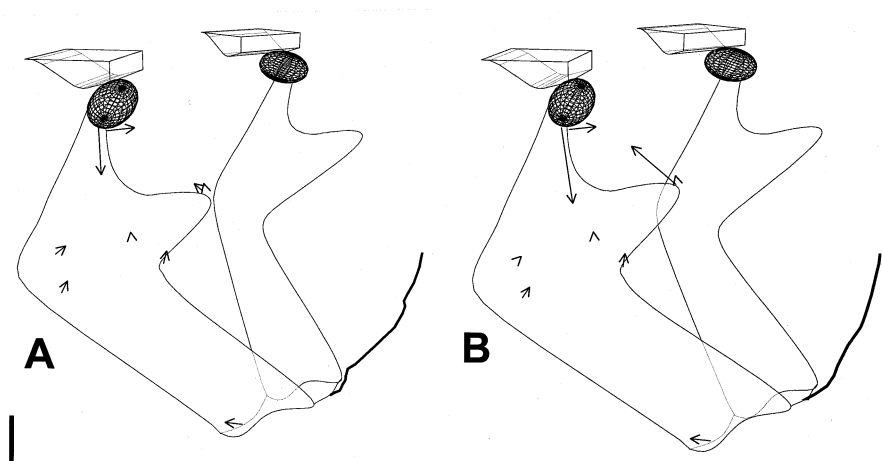


Fig. 7. Effect of simple and expanded linear jaw-opener muscle activity on incisor opening pathway for 25° condylar guidance models. Anterolateral view of (A) model 25LF, and (B) model 25XF including muscle vectors (right side only) at wide gape. Bold line represents mandibular incisor opening pathway. Calibration bar, 10 N (force vectors) or 12 mm (incisal displacement).

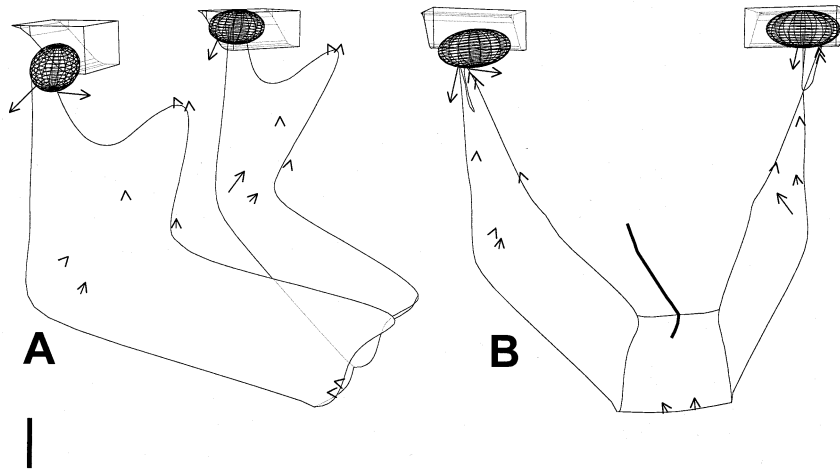


Fig. 8. Effect of simple linear, unilateral jaw-opener muscle activity (the left lateral pterygoid actuator has been removed) on incisor opening pathway for 40° condylar guidance model. (A) Anterolateral and (B) frontal views of model 40LF – As including muscle vectors at extreme lateral position. Bold line in frontal view represents mandibular incisor pathway. Calibration bar, 10 N (force vectors) or 12 mm (incisal displacement).

with values less than 2.4 N (Fig. 10c; Table 3). These passive tensions were maximal just before wide gape (superficial and deep masseter, and medial pterygoid tensions) or at wide gape (anterior, middle and posterior temporalis tensions). Condylar loading increased as the jaw opened and peaked at 10.0 N at wide gape (Fig. 12; Table 3).

As this model deviated by more than $\pm 0.5^\circ/\text{mm}$ from our objective of $2^\circ/\text{mm}$ at various points along the opening path, we subsequently selectively added more digastric or lateral pterygoid actuator activity to the simple linear force functions (model 25XF). The resulting jaw trajectory can be seen in Fig. 7. The final optimized, expanded linear functions for the lateral pterygoid and digastric actuators are outlined in Table 4 and Fig. 9b. Here, a gape of 48 mm was attained in 0.68 s, with the digastric and lateral pterygoid actuators reaching maximal forces of 3.4 and 6.4 N, respectively. Apart from the passive tension of 12.2 N in the posterior temporalis at wide gape, all passive muscle tensions remained below 2.0 N throughout the opening movement (Fig. 10d; Table 3). Superficial and deep masseter, medial pterygoid and anterior temporalis actuators reached their maximal tensions just before wide gape, whereas the middle and posterior temporalis actuators reached their maxima at wide gape. The TMJs were compressively loaded throughout the opening movement: joint forces increased to a maximum of 10.7 N at 40 mm and then increased sharply to 17.9 N at wide gape (Fig. 12), and followed the general form of passive

tensions in superficial and deep masseter, medial pterygoid and anterior temporalis actuators.

3.6. Asymmetrical opening

Plausible eccentric jaw opening (Fig. 8) was obtained by simply deactivating the left-sided lateral pterygoid actuator and activating the right-sided lateral pterygoid and bilateral digastric actuators with the simple linear functions from model 40LF (Fig. 9a). In this case, the jaw opened, and moved to its extreme lateral position, in 0.6 s, such that the mandibular incisor was displaced 21 mm inferiorly and 11 mm laterally. At this position, apart from tension in the left (ipsilateral) medial pterygoid (which rose sharply to 4.5 N as the model approached this extreme lateral position), passive tensions in all left-side muscles were lower than in right-side muscles (Fig. 13; Table 3). Both condyles were compressively loaded throughout the movement, although unevenly so, with maxima for the right and left condyles of 7.3 (contralateral) and 4.1 N (ipsilateral), respectively (Fig. 12; Table 3). The condyles remained in stable positions despite the absence of 'ligaments' or any other constraints (Figs. 10–12).

After reaching its most lateral position, the jaw commenced a medial movement while continuing to displace inferiorly (Fig. 8). At this time, the left condyle began to move anteroinferiorly along the posterior wall of the eminence. The passive tension in the left medial pterygoid remained around 4.5 N, while tensions in the other closers remained fairly constant or gradually increased (Fig. 13).

4. Discussion

4.1. Modeling assumptions

Computer models have been used widely to study muscle tensions, skeletal forces, motions, stresses, and strains in the back, lower limb, shoulder, elbow and jaw (e.g. Hawkins, 1992; McGill, 1992; van der Helm et al., 1992; Kuo and Zajac, 1993; Gonzales et al., 1993; Koriath and Hannam, 1994b; Osborn, 1996; Koolstra and van Eijden, 1997a,b). All such models are simpler than the systems they emulate, and ours is no exception, for it includes a rigid mandible, a fixed hyoid bone, and single-line actuators instead of complex muscles. In addition, we were forced to estimate many unknown muscle and inertial variables. Other variables were simplified to permit workable mathematical solutions and computation times (Table 1). We suggest our assumption of mandibular rigidity was reasonable, as skeletal distortion during jaw motion is reportedly less than 1.5 mm at the first molar (de Marco and Paine, 1974). We also consider our treatment of articular disc and fossa restraint as a single, compressible surface boundary against which the condyle functioned as rea-

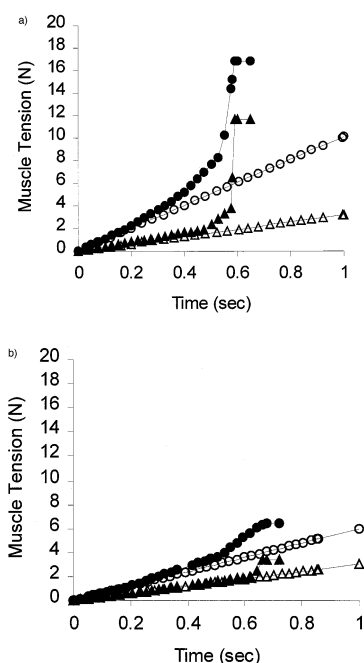


Fig. 9. Jaw-opener tensions plotted against time for (A) 40° condylar guidance models, 40LF and 40XF and (B) 25° condylar guidance models, 25LF and 25XF. Digastric tensions represented by circles (open circles denote simple linear functions, filled circles denote expanded linear functions). Lateral pterygoid tensions represented by triangles (open triangles denote simple linear functions, filled triangles denote expanded linear functions).

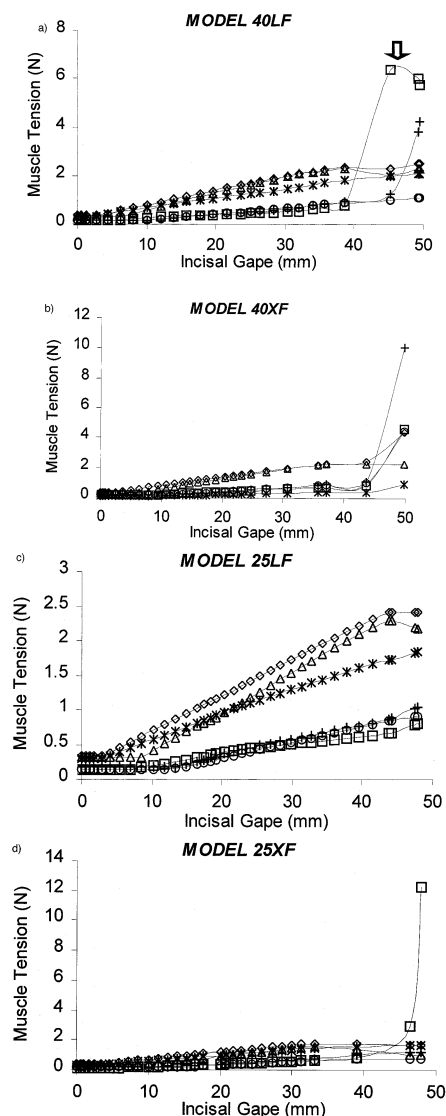


Fig. 10. Passive muscle tensions plotted against incisal gap during jaw opening in, (A) model 40LF; (B) model 40XF; (C) model 25LF; and (D) model 25XF. Legend, \diamond , superficial masseter; \circ , deep masseter; \triangle , medial pterygoid; *, anterior temporalis; +, middle temporalis; \square , posterior temporalis.

sonable in context; modeling a separate articular disc during jaw opening was not computationally practicable, as it would have required combining large-motion, rigid-body mechanics with flexible-structure, finite-element modeling. While finite-element modeling has provided valuable insight into static jaw mechanics (Koriath and Versluis, 1997), only Chen and Xu (1994) seem to have attempted dynamic finite-element modeling within the jaw. In their study, which was localized to the mandibular joint, a two-dimensional model was driven with joint-motion data. Although the magnitudes of condylar reaction forces and discal stresses in

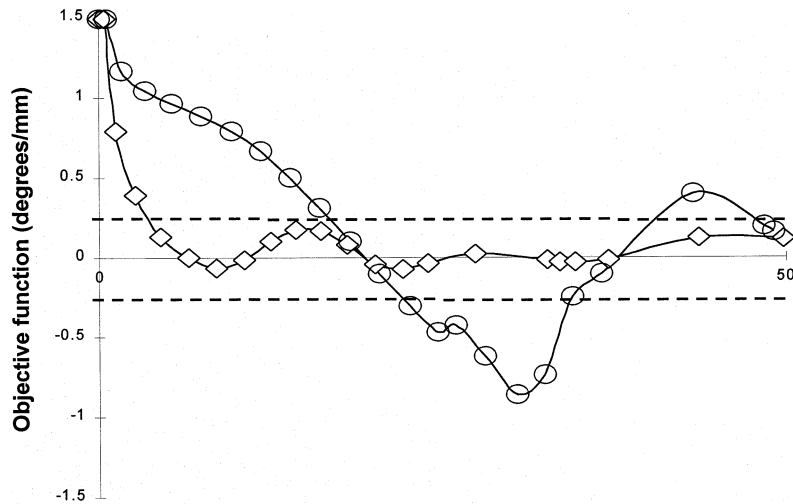


Fig. 11. Representative plots of objective functions (condylar rotation/translation, $-2^{\circ}/\text{mm}$) against incisal gape during jaw opening. Objective function denoted by circles results from jaw opening with simple linear jaw-opener muscle activity (model 40LF). Objective function denoted by diamonds results from jaw opening with expanded linear jaw-opener muscle activity (model 40XF). Note that objective function values greater than 0 indicate increased condylar rotation; conversely values below 0 indicate increased condylar translation [abscissa, incisal gape (mm)].

this instance were very sensitive to small alterations in joint motion, stress distributions in the disc remained relatively unchanged.

We fixed the position of the hyoid relative to the mandible, with the lines of action of the digastric muscles approximately 15° relative to the lower border of the mandible. The hyoid changes position during function (Winnberg, 1987; Winnberg et al., 1988; Haralabakis et al., 1993; Hiiemae et al., 1995), but its range of motion is not great, and in any event data on its position at maximum gape are sparse. Though the actions of the digastric muscle in relation to the hyoid apparatus were not the focus of this study, we have demonstrated previously that digastric and lateral pterygoid actuators move the jaw on surprisingly similar trajectories to maximum gape whether or not the hyoid is depressed (Langenbach et al., 1996). Hyoid motion would have had a negligible effect on jaw-closing muscle tensions. While hyoid depression must, of course, change the digastric's angle of attack (requiring a minor compensatory change in lateral pterygoid drive to maintain a given incisor-point trajectory), we consider that its omission did not detract significantly from our conclusions, especially those related to the maximum gape evoked (in the absence of muscle contraction) by an external force applied to the lower incisor region.

Our simplification of the multipennate jaw-closing muscles as sets of single-line actuators was clearly not ideal. The human masseter alone contains at least five, interleaved, aponeurotic septa running at various angles and it can contract regionally (van Eijden et al., 1993;

Hannam and McMillan, 1994). Nevertheless, we are unaware of a better method for simulating internal fibre and tendon mechanics in complex muscles, and our approach is consistent with recent work by others on jaw-muscle dynamics (Koolstra and van Eijden, 1997a,b). The actuators that we used produced tensions proportional to each muscle's regional cross-sectional area, and they incorporated jaw-muscle fibre-tendon ratios consistent with those in the literature. Also, in the case of the masseter and temporalis, several actuators operated between attachment sites within the same muscle. They simulated different amounts of regional stretch and the changing action lines dictated by the wide insertions of these muscles.

Our specification of maximal muscle lengths in the jaw closers as those at wide gape differed from those

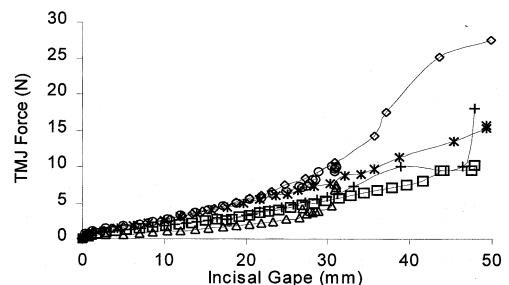


Fig. 12. TMJ loads plotted against incisal gape during jaw opening in, *, model 40LF; \diamond , model 40XF; \square , model 25LF; +, model 25XF; \circ , model 40 – As-right TMJ; \triangle , model 40 – As-left TMJ.

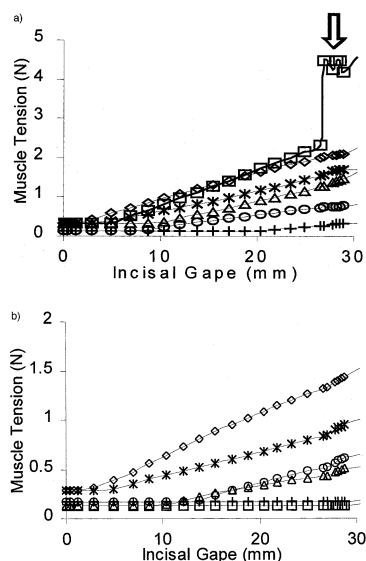


Fig. 13. Passive muscle tensions plotted against incisal gap during asymmetric opening in model 40LF – As. (A) Tensions in masseter and medial pterygoid muscle groups. \diamond , Right superficial masseter; \circ , right deep masseter; \triangle , right medial pterygoid; $*$, left superficial masseter; $+$, left deep masseter; \square , left medial pterygoid. (B) Tensions in temporalis muscle groups. \diamond , Right anterior temporalis; \circ , right middle temporalis; \triangle , right posterior temporalis; $*$, left anterior temporalis; $+$, left middle temporalis; \square , left posterior temporalis.

used in other recent models (Koolstra and van Eijden, 1995, 1996, 1997a,b). Our maximal muscle stretch invariably occurred at 150% optimal muscle-fibre length and was uniform for all closing muscles. In vivo, however, it is possible that different individuals of stretch occur among the different muscles at maximum gap (and indeed in the same muscle among different individuals) (Brown et al., 1996). The tension correlates for such length changes in living human jaw muscles are, however, not reported, and it is difficult to visualize an experiment that could reveal them. While the complexities of internal organization may evoke changes in fibre length which differ from those that we assumed, it remains possible that the overall behavior of each muscle as a whole approximates that of our actuator (or actuator sets). We speculate, however, that the system more probably includes fibre and whole-muscle length–tension characteristics unique to each muscle.

Notwithstanding these reservations, we propose that the more models display behavioral characteristics that mimic those known in vivo, the more plausible they become (Zajac, 1989), in this case providing a starting point for appraising what must be achieved by functioning human jaw muscles and for experimenting with their properties. Viewed this way, our model predicted realistic spatial variables for jaw opening caused by openers working against passive tensions in closers.

4.2. Muscle tensions

By definition, maximum active muscle tension in each of our closers would develop at incisal gaps between 4 and 10 mm. Collectively, the muscles' optimal lengths occurred at different gaps, which, if true, suggests that the masticatory system is able to produce relatively large forces over a useful range of gaps. This gap at which the optimal length of the closers occurs is lower than the reported incisal gap of between 13 and 21 mm when maximum molar bite force is produced (Manns et al., 1979; Mackenna and Turker, 1983). However, our actuators had defined optimal muscle fibre lengths of two-thirds of the maximal fibre length, as this produced the maximum fibre stretch that skeletal muscle is believed to undergo (Brown et al., 1996). If we reduced our assumed relative fibre stretch (which may indeed occur), then our optimal fibre length would be set at a wider gap and agree more closely with values reported in the literature. By altering the model in this way, however, our rest position without activity in the jaw closers would occur at an even wider gap, requiring more closing muscle tone to maintain a clinical rest position of 3–5 mm.

We were somewhat surprised that a force of only 5 N was needed to open the jaw widely in living persons, though this confirmed earlier work in which a similar, low force of 0.65 kg (6.4 N) was reported (Lynn and Yemm, 1971). Low passive resistance has also been found in the rat tibialis, where minimal passive tensions were generated within the muscles' normal range of motion (Hawkins and Bey, 1997). We consider that our passive resistance was due mainly to passive muscle resistance, though some voluntary muscle activity and involuntary reflexes could have contributed (see Hanam and Sessle, 1994). The rigorous requirement that the model should meet this experimentally derived specification, i.e. that the passive tensions of the closer actuators should permit wide gap with a 5-N external force, differs from previous work. Others have assigned passive tension properties to the closing muscles by calculating the tensions as an exponential function of sarcomere length (Koolstra and van Eijden, 1997a,b). These models were unable to attain interincisal distances > 35 mm. Although this limited gap (at least in one study) was attributed in part to incorrect jaw-opener tensions at wide gap (Koolstra and van Eijden, 1997b), an attractive alternative explanation is that the passive tensions in the jaw closers were too high. In these limited-gap studies, a one-to-one relation between sarcomere length and whole-muscle length change was used. For pennated muscles such as the jaw closers, however, change in sarcomere length represents approximately 70% of the length change in the whole muscle (Muhl, 1982; van Ruijven and Weijts, 1990). If this ratio were used in these studies, passive muscle

forces would be expected to be lower than those reported. In addition, the values used in an exponential function to compute passive muscle tensions were derived from adult rabbits. As the passive muscle-tension properties of young and adult rabbits (Weijts et al., 1989) and rats (Woittiez et al., 1986) differ, they may also be dissimilar from those in humans. In any event if, as our study suggests, relatively low passive muscle tensions are induced during wide jaw opening, lower passive forces must be evoked at or near tooth contact; thus the passive tensions induced during acts such as mastication would be far smaller than the active tensions generated by the closing muscles. This implies that they may have little constraining effect on the trajectories of jaw motion during such functions.

The model behaved in a stable manner during asymmetric jaw opening, during which it required no modification of the passive tension properties of closing muscles. This reinforces our impression that complex masticatory muscle behavior can be represented, albeit crudely, with multiple actuators.

4.3. Mandibular rest position

The gape requirements of the model meant that active closer-muscle tensions were needed to maintain a plausible mandibular resting posture. Our inability to find length–tension curves that simultaneously satisfied the twin criteria of maximum gape with a 5-N force applied to the jaw and a normal clinical ‘rest position’ of 3–5 mm incisal separation implies that low-level muscle activity is indeed needed to establish the freeway space in the awake individual. This idea is not new, as it is consistent with previous studies on the plasticity of the position and its dependence on alertness (Yemm, 1976; Rugh and Johnson, 1984). It is notable that the additional tension needed in the closers was very low, and did not restrict muscle-driven jaw opening when left ‘on’.

4.4. Jaw opening

Normally, jaw opening includes coactivation of digastric and lateral pterygoid muscles. Matching jaw motions induced by our digastric and lateral pterygoid actuators were chiefly sagittal-plane rotation and anterior jaw translation, respectively (Langenbach and Hannam, 1999). Digastric activity (complemented by gravity) overcame the predominantly upward directed jaw-closer passive tensions and lateral pterygoid activity caused anterior translation of the jaw, with wide opening at a rate of 2° sagittal-plane jaw rotation per mm of anterior condylar translation. The active tensions in these muscles increased with time, so active jaw opening occurred over 1 s. The digastric and lateral pterygoid actuators reached a maximum of 11.6 and

16.8 N, respectively, which equates to approximately 30 and 25% of their respective F_{\max} (Table 3). Although the maximum tension a muscle is able to generate depends on its length and velocity (Zajac, 1989), these correlations were not incorporated into our actuators as their tensions never approached F_{\max} . Presumably F_{\max} would be reached in these muscles during jaw opening against resistance, in which case the active length–tension and velocity–tension correlations would have to be considered.

As we had specific constraints, such as a predefined jaw rotation/translation ratio and opening duration, on our jaw model we were able to obtain a unique solution for active tensions in the lateral pterygoid and digastric muscles. In a less constrained system, and in vivo, this unique solution could be replaced by many different muscle-activation strategies for the same task.

4.5. Articular loading

Direct studies in mammals suggest that the TMJ is compressively loaded during function (Hylander, 1985; Boyd et al., 1990; Nitzan, 1994), but there is some disagreement about when and where maximum articular loads occur (Hylander, 1985; Boyd et al., 1990). Direct experimental measurement of articular loading is sparse (Hylander, 1979, 1985; Boyd et al., 1990; Nitzan, 1994; Marks et al., 1997), though articular loads ranged between 6 and 175 N for chewing, drinking and aggressive vocalization in the monkey (Boyd et al., 1990).

In our model, increasing compressive loading of both condyles took place during the entire phase of midline and eccentric opening, and consequently might be expected to maintain continual apposition of condyle, disc and fossa if its predictions apply in vivo (Fig. 12). Maximum loads of 28 N occurred during midline opening in our model with steeper (40°) condylar guidance. This value is less than that reported in another study (approximately 75 N posteriorly directed and 110 N inferiorly directed forces in relation to the mandibular center of gravity (Koolstra and van Eijden, 1997b)). One explanation is that our activation of the jaw openers was significantly less than the 100% used in that work. It is particularly interesting that during the eccentric jaw opening caused by right-sided lateral pterygoid action and bilateral digastric activity, both condyles sustained compressive (though uneven) loads, and remained in apposition with the articular restraints despite the absence of ‘ligaments’.

The apparent appositional functioning within our model’s two articulations during widely excursive tasks reinforces our impression that, for these acts at least, muscle tensions are a prime factor in maintaining articular integrity during function.

5. Conclusions

Movements such as jaw opening involve a complex interaction between passive muscle tensions, active muscle tensions and craniofacial form. Here, we were able to simulate plausible midline and eccentric jaw opening by utilizing available morphological and functional data in a three-dimensional mathematical model. This model required active tone in the jaw closers to maintain a simulated clinical rest position. Our results suggest that, for these tasks, jaw function can be maintained in the absence of ligaments and occurs in the presence of compressive articular loading. Tensions in the jaw openers and jaw closers, and the resultant articular forces, remained reasonably low and would presumably increase if resistance to motion were encountered. We suggest that virtual approaches to craniofacial biomechanics, such as that used here, enable investigation of correlations between structure and function which are otherwise impossible to disclose, and serve as constructs for hypotheses driving future human and animal experiments.

References

- ADAMS, 1994. ADAMS optimization guide, version 8.0 ed. Mechanical Dynamics, Ann Arbor.
- Baron, P., Debussy, T., 1979. A biomechanical functional analysis of the masticatory muscles in man. *Arch. Oral Biol.* 24, 547–553.
- Boyd, R.L., Gibbs, C.H., Mahan, P.E., Richmond, A.F., Laskin, J.L., 1990. Temporomandibular joint forces measured at the condyle of *Macaca arctoides*. *Am. J. Orthodontics Dentofacial Orthop.* 97, 472–479.
- Brill, N., Tryde, G., 1974. Physiology of mandibular positions. In: Kawamura, Y. (Ed.), *Frontiers of Oral Physiology: Physiology of Mastication*. S. Karger, Basel, p. 199.
- Brown, I.E., Liinamaa, T.L., Loeb, G.E., 1996. Relationships between range of motion, L_{00} , and passive force in five strap-like muscles of the feline hind limb. *J. Morphol.* 230, 69–77.
- Carlsson, G.E., LeResche, L., 1995. Epidemiology of temporomandibular disorders. In: Sessle, B.J., Bryant, P.S., Dionne, R.A. (Eds.), *Temporomandibular Disorders and Related Pain Conditions*. IASP Press, Seattle, pp. 211–226.
- Chen, J., Xu, L., 1994. A finite element analysis of the human temporomandibular joint. *J. Biomech. Eng.* 114, 401–407.
- Creanor, S.L., Noble, H.W., 1994. Comparative functional anatomy. In: Zarb, G.A., Carlsson, G.E., Sessle, B.J., Mohl, N.D. (Eds.), *Temporomandibular Joint and Masticatory Muscle Disorders*. Munksgaard, Copenhagen, pp. 17–47.
- Curwin, S., Stanish, W.D., 1984. *Tendonitis: Its Etiology and Treatment*. Collamore Press, Lexington.
- de Marco, T., Paine, S., 1974. Mandibular dimensional change. *J. Prosthet. Dent.* 31, 482–485.
- Dechow, P.C., Nail, G.A., Schwartz-Dabney, C.L., Ashman, R.B., 1993. Elastic properties of human supraorbital and mandibular bone. *Am. J. Phys. Anthropol.* 90, 291–306.
- Dibdin, G.H., Griffiths, M.J., 1975. An intra-oral telemetry system for the continuous recording of vertical jaw movement. *Phys. Med. Biol.* 20, 355–365.
- Fitts, R.H., McDonald, K.S., Schluter, J.M., 1991. The determinants of skeletal muscle force and power: their adaptability with changes in activity pattern. *J. Biomech.* 24 (Suppl. 1), 111–122.
- Gonzales, R.V., Andritsos, M.J., Barr, R.E., Abraham, L.D., 1993. Comparison of experimental and predicted muscle activation patterns in ballistic elbow movements. *Biomed. Sci. Instrum.* 29, 9–16.
- Gordon, A.M., Huxley, A.F., Julian, F.J., 1966. The variation in isometric tension with sarcomere length in vertebrate muscle fibres. *J. Physiol.* 184, 170–192.
- Goto, T.K., Langenbach, G.E.J., Koriath, T.W.P., Hagiwara, M., Tonndorf, M.L., Hannam, A.G., 1995. Functional movements of putative jaw muscle insertions. *Anat. Rec.* 242, 278–288.
- Hannam, A.G., McMillan, A.S., 1994. Internal organization in the human jaw muscles. *Crit. Rev. Oral Biol. Med.* 5, 55–89.
- Hannam, A.G., Sessle, B.J., 1994. Temporomandibular neuromuscular physiology. In: Zarb, G.A., Carlsson, G.E., Sessle, B.J., Mohl, N.D. (Eds.), *Temporomandibular Joint and Masticatory Muscle Disorders*. Munksgaard, Copenhagen, pp. 67–100.
- Hannam, A.G., Langenbach, G.E.J., 1995. Modelling the masticatory system during function. In: Morimoto, T., Matsuya, T., Takada, K. (Eds.), *Brain and Oral Functions Oral Motor Function and Dysfunction*. Elsevier, Amsterdam, pp. 217–226.
- Haralabakis, N.B., Toutountzakis, N.M., Yiagtzis, S.C., 1993. The hyoid bone position in adult individuals with open bite and normal occlusion. *Eur. J. Orthodontics* 15, 265–271.
- Hawkins, D., 1992. Software for determining lower extremity muscle-tendon kinematics and moment-arm length during flexion/extension movements. *Comput. Biol. Med.* 22, 59–71.
- Hawkins, D., Bey, M., 1997. Muscle and tendon force-length properties and their interactions in vivo. *J. Biomech.* 30, 63–70.
- Hiimae, K.M., Hayenga, S.M., Reese, A., 1995. Patterns of tongue and jaw movement in a cinefluorographic study of feeding in the macaque. *Arch. Oral Biol.* 40, 229–246.
- Hill, A.V., 1953. Mechanics of active muscle. *Proc. R. Soc. London* 141, 104–117.
- Hylander, W.L., 1979. Experimental analysis of temporomandibular joint reaction force in macaques. *Am. J. Phys. Anthropol.* 51, 433–456.
- Hylander, W.L., 1985. Mandibular function and temporomandibular joint loading. In: Carlson, D.S., McNamara, J.A. Jr, Ribbens, K.A. (Eds.), *Developmental Aspects of Temporomandibular Joint Disorders*. University of Michigan, Ann Arbor, pp. 19–35.
- Ikai, M., Fukunaga, T., 1968. Calculation of muscle strength per unit cross-sectional area of human muscle by means of ultrasonic measurement. *Internationale Zeitschrift Angewandte Physiologie Einschliesslich Arbeitsphysiologie* 26, 26–32.

- Kawamura, Y., Kato, I., Takata, M., 1967. Jaw-closing muscle activities with the mandible in rest position. *J. Dent. Res.* 46, 1356–1362.
- Koolstra, J.H., van Eijden, T.M., 1995. Biomechanical analysis of jaw-closing movements. *J. Dent. Res.* 74, 1564–1570.
- Koolstra, J.H., van Eijden, T.M., 1996. Influence of the dynamical properties of the human masticatory muscles on jaw closing movements. *Eur. J. Morphol.* 34, 11–18.
- Koolstra, J.H., van Eijden, T.M., 1997a. Dynamics of the human masticatory muscles during a jaw open–close movement. *J. Biomech.* 30, 883–889.
- Koolstra, J.H., van Eijden, T.M., 1997b. The jaw open–close movements predicted by biomechanical modelling. *J. Biomech.* 30, 943–950.
- Korioth, T.W., Hannam, A.G., 1994a. Deformation of the human mandible during simulated tooth clenching. *J. Dent. Res.* 73, 56–66.
- Korioth, T.W., Hannam, A.G., 1994b. Mandibular forces during simulated tooth clenching. *J. Orofacial Pain* 8, 178–189.
- Korioth, T.W., Versluis, A., 1997. Modeling the mechanical behaviour of the jaws and their related structures by finite element (FE) analysis. *Crit. Rev. Oral Biol. Med.* 8, 90–104.
- Kuo, A.D., Zajac, F.E., 1993. Human standing posture: multi-joint movement strategies based on biomechanical constraints. *Prog. Brain Res.* 97, 349–358.
- Langenbach, G.E.J., Hannam, A.G., 1999. The role of passive muscle tensions in a three-dimensional dynamic model of the human jaw. *Arch. Oral Biol.* 44, 557–573.
- Langenbach, G.E.J., Peck, C.C., Hannam, A.G., 1996. Predicted tensions in human jaw muscles during function. *J. Dent. Res.* 75 (SI), #1590 (abstract).
- Lundeen, H.C., Shryock, E.F., Gibbs, C.H., 1978. An evaluation of mandibular border movements: their character and significance. *J. Prosthet. Dent.* 40, 442–452.
- Lynn, A.M.J., Yemm, R., 1971. External forces required to move the mandible of relaxed human subjects. *Arch. Oral Biol.* 16, 1443–1447.
- Mackenna, B.R., Turker, K.S., 1983. Jaw separation and maximum incising force. *J. Prosthet. Dent.* 49, 726–730.
- Manns, A., Miralles, R., Palazzi, C., 1979. EMG, bite force, and elongation of the masseter muscle under isometric voluntary contractions and variations of vertical dimension. *J. Prosthet. Dent.* 42, 674–682.
- Marks, L., Teng, S., Årtun, J., Herring, S., 1997. Reaction strains on the condylar neck during mastication and maximum muscle stimulation in different condylar positions: an experimental study in the miniature pig. *J. Dent. Res.* 76, 1412–1420.
- McGill, S.M., 1992. A myoelectrically-based dynamic three-dimensional model to predict loads on lumbar spine tissues during lateral bending. *J. Biomech.* 25, 395–414.
- McNamara, J.A. Jr, 1974. Electromyography of the mandibular resting posture position in the rhesus monkey (*macaca mulatta*). *J. Dent. Res.* 53, 945.
- Miller, A.J., Chierici, G., 1977. The bilateral response of the temporal muscle in the rhesus monkey (*macaca mulatta*) to short-term detachment of the muscle and increased loading of the mandible. *J. Dent. Res.* 56, 1620–1628.
- Møller, E., 1976. Evidence that the rest position is subject to servo-control. In: Anderson, D.J., Matthews, B. (Eds.), *Mastication*. John Wright, Bristol, pp. 72–80.
- Muhl, Z.F., 1982. Active length tension relation and the effect of muscle pinnation on fiber lengthening. *J. Morphol.* 173, 285–292.
- Muhl, Z.F., Grimm, A.F., Glick, P.L., 1978. Physiologic and histologic measurements of the rabbit digastric muscle. *Arch. Oral Biol.* 23, 1051–1059.
- Muto, T., Kanazawa, M., 1994. Positional change of the hyoid bone at maximal mouth opening. *Oral Surg. Oral Med. Oral Pathol. Oral Radiol. Endodontics* 77, 451–455.
- Nelson, G.J., 1986. Three dimensional computer modeling of human mandibular biomechanics. Thesis, The University of British Columbia, Vancouver, Canada.
- Nitzan, D.W., 1994. Intraarticular pressure in the functioning human temporomandibular joint and its alteration by uniform elevation of the occlusal plane. *J. Oral Maxillofac. Surg.* 52, 671–679.
- Nygaard, E., Houston, M., Suzuki, Y., Jorgensen, K., Saltin, B., 1983. Morphology of the brachial biceps muscle and elbow flexion in man. *Acta Physiol. Scand.* 117, 219–226.
- Öberg, T., Carlsson, G.E., Fajers, C.M., 1971. The temporomandibular joint: a morphologic study on a human autopsy material. *Acta Odontol. Scand.* 29, 349–383.
- Oishi, T., 1967. A study on the anatomical structure of temporomandibular joint from the standpoint of mandibular movement. *J. Jpn. Prosthodontic Soc.* 11, 197–220.
- Osborn, J.W., 1996. Features of human jaw design which maximize the bite force. *J. Biomech.* 29, 589–595.
- Pancherz, H., Winnberg, A., Westesson, P.L., 1986. Masticatory muscle activity and hyoid bone behaviour during cyclic jaw movements in man. *Am. J. Orthodontics Dentofacial Orthop.* 89, 122–131.
- Peck, C.C., Murray, G.M., Johnson, C.W.L., Klineberg, I.J., 1997. The variability of condylar point pathways in open–close jaw movements. *J. Prosthet. Dent.* 77, 394–404.
- Posselt, U., 1952. Studies in the mobility of the human mandible. *Acta Odontol. Scand.* 10, 1–151.
- Posselt, U., 1968. *Physiology of Occlusion and Rehabilitation*, second ed. Blackwell, Oxford.
- Pruim, G., de Jongh, H.J., Ten Bosch, J., 1980. Forces acting on the mandible during bilateral static bite at different bite force levels. *J. Biomech.* 13, 755–763.
- Rugh, J.D., Johnson, R.W., 1984. Vertical dimension discrepancies and masticatory pain/dysfunction. In: Solberg, W.K., Clark, G.T. (Eds.), *Abnormal Jaw Mechanics: Diagnosis and Treatment*. Quintessence, Chicago, pp. 117–133.
- Salaorni, C., Palla, S., 1994. Condylar rotation and anterior translation in healthy human temporomandibular joints. *Schweiz. Monatsschrift Zahnmedizin* 104, 415–422.
- Solberg, W.K., Hansson, T.L., Nordstrom, B., 1985. The temporomandibular joint in young adults at autopsy: a morphologic classification and evaluation. *J. Oral Rehabil.* 12, 303–321.
- Storey, A., 1995. Biomechanical and anatomical aspects of the temporomandibular joint. In: Sessle, B.J., Bryant, P.S., Dionne, R.A. (Eds.), *Temporomandibular Disorders and Related Pain Conditions*. IASP Press, Seattle, pp. 257–272.

- Szentpetery, A., 1993. Clinical utility of mandibular movement ranges. *J. Orofacial Pain* 7, 163–167.
- van den Bogert, A.J., Nigg, B.M., 1999. Simulation. In: Nigg, B.M., Herzog, W. (Eds.), *Biomechanics of the Musculoskeletal System*. Wiley, Chichester, pp. 594–616.
- van der Helm, F.C., Vergeer, H.E., Pronk, G.M., van der Woude, L.H., Rozendal, R.H., 1992. Geometry parameters for musculoskeletal modelling of the shoulder system. *J. Biomech.* 25, 129–144.
- van Eijden, T.M., Raadsheer, M.C., 1992. Heterogeneity of fiber and sarcomere length in the human masseter muscle. *Anat. Rec.* 232, 78–84.
- van Eijden, T.M., Blanksma, N.G., Brugman, P., 1993. Amplitude and timing of EMG activity in the human masseter muscle during selected motor tasks. *J. Dent. Res.* 72, 599–606.
- van Eijden, T.M., Koolstra, J.H., Brugman, P., 1995. Architecture of the human pterygoid muscles. *J. Dent. Res.* 74, 1489–1495.
- van Eijden, T.M., Koolstra, J.H., Brugman, P., 1996. Three-dimensional structure of the human temporalis muscle. *Anat. Rec.* 246, 565–572.
- van Eijden, T.M., Korfage, J.A.M., Brugman, P., 1997. Architecture of the human jaw-closing and jaw-opening muscles. *Anat. Rec.* 248, 464–474.
- van Ruijven, L.J., Weijs, W.A., 1990. A new model for calculating forces from electromyograms. *Eur. J. Appl. Physiol. Occup. Physiol.* 61, 479–485.
- Weijs, W.A., Hillen, B., 1984a. Relationship between the physiological cross-section of the human jaw muscles and their cross-sectional area in computer tomograms. *Acta Anat.* 118, 129–138.
- Weijs, W.A., Hillen, B., 1984b. Relationships between masticatory muscle cross-section and skull shape. *J. Dent. Res.* 63, 1154–1157.
- Weijs, W.A., Hillen, B., 1985. Physiological cross-section of the human jaw muscles. *Acta Anat.* 121, 31–35.
- Weijs, W.A., Korfage, J.A., Langenbach, G.E.J., 1989. The functional significance of the position of the centre of rotation for jaw opening and closing in the rabbit. *J. Anat.* 162, 133–148.
- Winnberg, A., 1987. Suprahyoid biomechanics and head posture. An electromyographic, videofluorographic and dynamographic study of hyo-mandibular function in man. *Swedish Dent. J. Suppl.* 46, 1–173.
- Winnberg, A., Pancherz, H., Westesson, P.L., 1988. Head posture and hyo-mandibular function in man. A synchronized electromyographic and videofluorographic study of the open–close–clench cycle. *Am. J. Orthodontics Dentofacial Orthop.* 94, 393–404.
- Winters, J.M., 1990. Hill-based muscle models: a systems engineering perspective. In: Winters, J.M., Woo, S.L.-Y. (Eds.), *Multiple Muscle Systems: Biomechanics and Movement Organization*. Springer, New York, pp. 69–93.
- Woittiez, R.D., Huijting, P.A., Rozendal, R.H., 1983. Influence of muscle architecture on the length–force diagram of mammalian muscle. *Pflug. Arch. Eur. J. Physiol.* 399, 275–279.
- Woittiez, R.D., Heerkens, Y.F., Huijting, P.A., Rijnsburger, W.H., Rozendal, R.H., 1986. Functional morphology of the m.gastrocnemius medialis of the rat during growth. *J. Morphol.* 187, 247–258.
- Wong, M., Carter, D.R., 1988. Mechanical stress and morphogenetic endochondral ossification of the sternum. *J. Bone Jt. Surg.* 70-A, 992–1000.
- Yale, S.H., Allison, B.D., Hauptfuehrer, J.D., 1966. An epidemiological assessment of mandibular condyle morphology. *Oral Surg. Oral Med. Oral Pathol. Oral Radiol. Endodontics* 21, 169–177.
- Yemm, R., 1976. The role of tissue elasticity in the control of mandibular resting posture. In: Anderson, D.J., Matthews, B. (Eds.), *Mastication*. John Wright, Bristol, pp. 81–89.
- Zajac, F.E., 1989. Muscle and tendon: properties, models, scaling, and application to biomechanics and motor control. *Crit. Rev. Biomed. Eng.* 17, 359–411.